

Wide Dynamic-Range Beam-Profile Instrumentation For A Beam-Halo Measurement: Description And Operation*

J. Douglas Gilpatrick*,

** Los Alamos National Laboratory, MS H808, LANL, Los Alamos, NM, 87545*

Abstract. Within the halo experiment conducted at the Low Energy Demonstration Accelerator (LEDA) at LANL, specific beam instruments that acquire horizontally and vertically projected particle-density distributions out to $> 100000:1$ dynamic range are located throughout the 52-magnet halo lattice. We measured the core of the distributions using traditional wire scanners, and the tails of the distributions using water-cooled graphite scraping devices. The wire scanner and halo scrapers are mounted on the same moving frame whose location is controlled with stepper motors. A sequence within the Experimental Physics and Industrial Control System (EPICS) software communicates with a National Instruments LabVIEW virtual instrument to control the motion and location of the scanner/scrapper assembly. Secondary electrons from the wire scanner 0.033-mm carbon wire and protons impinging on the scraper are both detected with a lossy-integrator electronic circuit. Algorithms implemented within EPICS and in Research System's Interactive Data Language subroutines analyze and plot the acquired distributions. This paper describes the beam instrument and our experience with its operation.

INTRODUCTION

At LEDA, a 100-mA, 6.7-MeV beam is injected into a 52-quadrupole-magnet lattice (see Fig. 1). Within this 11-m FODO lattice, there are nine wire scanner/halo scraper (WS/HS) stations, five pairs of steering magnets and beam position monitors, five loss monitors, and three pulsed-beam current monitors [1]. The WS/HS instrument's purpose is to measure the beam's transverse projected distribution. These measured distributions must have sufficient detail to understand beam halo resulting from upstream lattice mismatches [2,3]. The first WS/HS station, located after the fourth quadrupole magnet, verifies the beam's transverse characteristics after the RFQ exit. A cluster of four WS/HS located after magnets #20, #22, #24, and #26 provides phase space information after the beam has debunched. After magnets #45, #47, #49, and #51 reside the final four WS/HS stations. These four WS/HS acquire projected beam distributions under both matched and mismatched conditions. These conditions are generated by adjusting the first-four quadrupole magnetic fields so that the RFQ output beam is matched or mismatched in a known fashion to the rest of the lattice. Because the halo

takes many lattice periods to fully develop, this final cluster of WS/HS are positioned to be most sensitive to halo generation.

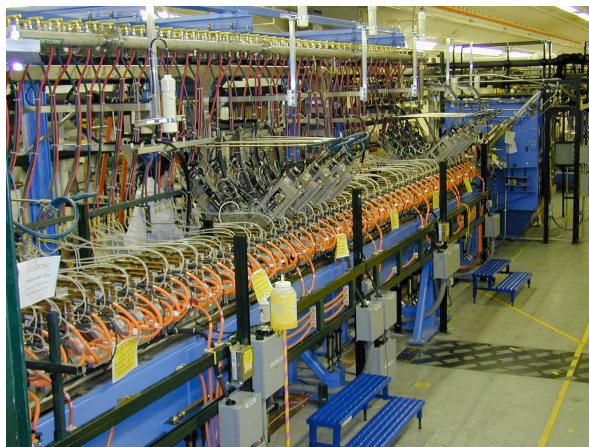


FIGURE 1. The 11-m, 52-magnet FODO lattice includes nine WS/HS stations that measure the beam's transverse projected distributions.

As the RFQ output beam is mismatched to the lattice, the WS/HS actually observe a variety of distortions to a properly matched Gaussian-like

* Work supported by the US Department of Energy.

distribution [2,3]. These distortions appear as distribution tails or backgrounds. It is the size, shape, and extent of these tails that predict specific types of halo. However, not every lattice WS/HS observes the halo generated in phase space because the resultant distribution tails may be hidden from the projection's view. Therefore, multiple WS/HS are used to observe the various distribution tails.

WS/HS DESCRIPTION

Each station consists of a horizontal and vertical actuator assembly (see Fig. 2) that can move a 33- μm -carbon monofilament and two graphite/copper scraper sub-assemblies. The carbon wire and scrapers are connected to the same movable frame. Attached to this movable frame is a linear encoder that provides the wire and scraper edges' relative position to within a typical rms error of 5 μm , and an additional linear potentiometer provides an absolute approximate position for LEDA's run-permit systems. A stepper motor coupled to a ball lead screw is used to drive the moveable frame. A motor-brake and micro-switches limit the frame's movement.

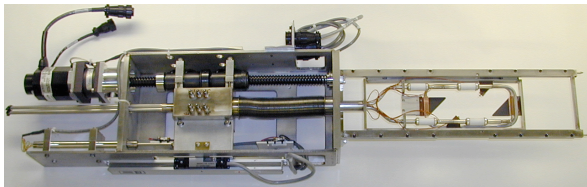


FIGURE 2. The WS/HS assembly contains a movable frame on which a 0.033-mm carbon wire resides between two water-cooled graphite scrapers.

The carbon wire, which senses the beam's core, is cooled by thermal radiation. If the beam macropulse is too long, the wire temperature continues above 1800 K resulting in the onset of thermionic emission. Thermionic emission causes an inaccurate appearance to the distribution by exaggerating the core's current density. To eliminate these effects for the halo experiment, the maximum pulse length and repetition rate is limited to approximately 30 μs and 1 Hz, respectively.

The halo scrapers are composed of a 1.5-mm thick graphite plate brazed to a water-cooled 1.5-mm thick copper plate. Since 6.7-MeV protons average range in carbon is approximate 0.3 mm, the beam is completely stopped within the graphite plate. Cooling via conduction lowers the average temperature of the scraper sub-assembly and allows the scraper to be

cooled more rapidly than the wire. The lower average temperature and faster cooling allows the scraper to be driven in as far as 2 rms widths from the beam distribution peak without the peak temperature increasing above 1800 K.

The movement and positioning of each wire and scraper pair is controlled by a motion control system that contains a stepper motor, stepper motor controller, a linear encoder, and an electronic driver amplifier. The controller's digital PID loop controls the speed and accuracy at which the assembly is moved and placed.

The target position, as defined by the WS/HS operator, is relayed from the EPICS control screen via a database process variable to a National Instruments LabVIEW Virtual Instrument (VI). The VI also calibrates the relative position of the linear encoders based on the measured position of the limit switches, and provides some error feedback information. The total error between the target wire position and the actual wire position attained is within a total 4% range of a typical 1-mm rms-width beam.

As the wire is moved through the beam, it senses the projected beam core distribution. A small portion of the beam's energy is imparted to the wire causing secondary electron emission to occur. The secondary electrons leaving the wire are replaced by negative charge flowing from the electronics. This current flow for both axes is connected through a bias battery to an electronic lossy integrator circuit and followed by an amplification stage.

The integrator capacitance and amplifier gain are set to allow a very wide range of values of accumulated charge. Data are acquired by digitizing the accumulated charge through the lossy integrator at two different times within the beam pulse. This charge difference, acquired by subtracting the two values of charge, provides a low noise method of relative beam charge acquisition. The wire and scraper accumulated charge signals are digitized using 12- and 14-bit digitizers, respectively. The analog noise floor has been measured to be 0.03 pC, a noise level slightly lower than the scraper digital LSB noise level of 0.15 pC using the highest gain settings within the detection electronics.

The front-end electronic circuitry, mounted on a daughter printed circuit board, is connected to a motherboard that has all of the necessary interface electronics to communicate with EPICS via a controller module within the same electronics crate. A software state machine sequence was written within

EPICS to control and operate WS/HS instrumentation. The state machine instructs the VI to move the wire and scraper to a specific location, acquire synchronous distribution data from either the wire or scraper, trigger the IDL routine to normalize the acquired charge with a nearby toroidal current measurement, graph the normalized data, and write the distribution to a file. The sequence also instructs IDL to calculate the first through fourth moments, fit a Gaussian distribution to the wire scanner data, and calculate the point at which the beam distribution disappears into the background noise.

To plot the complete beam distribution for each axis, the wire scanner and two scraper data sets must be joined. To accomplish this joining, several analysis tasks are performed on the wire and scraper data including, scraper data are spatially differentiated and averaged, wire and scraper data are acquired with sufficient spatial overlap, and differentiated scraper data are normalized to the wire beam core data.

The scraper data need only be normalized in the relative charge axis since the distances between each wire and scraper edge are known to within 0.25-mm. In addition, the first four moments and the point at which the beam distribution disappears into the noise are also calculated for the combined distribution data.

ACQUIRED DISTRIBUTIONS

Figs. 3 and 4 show typical data from the vertical and horizontal profiles from the WS/HS #51 under a matched and a mismatched condition. The projected distributions displayed in these two figures have had the axis offset displacement subtracted and have been normalized so that their integrals are equal. The matched condition was acquired by comparing all of the final eight WS/HS acquired profile root-mean-square (rms) beam widths and adjusting the first four quadrupole lattice magnets so that all eight beam widths in a single axis are equal. The initial-four quadrupole magnets fields were then adjusted to change the match so that the beam's mismatch parameter was increased by 50%.

Under specific beam mismatch conditions, additional “shoulders” develop in both horizontal and vertical profiles at this particular lattice location. While showing an increase, the rms beam width and full-width-half-maximum (FWHM) do not provide sufficient descriptive information of the beam profile changes. Since these shoulders are most pronounced between 1- to 10-% of the peak of the projected

distribution, further describing the distribution by comparing distribution values of full-width-10%-maximum (FW10%M) and full-width-1%-maximum (FW1%M) values was also very instructive. A more complete description of the matching process and the related beam physics can be obtained from references written by Wangler and Colestock [2,3].

The typical profiles acquired by the WS/HS show distributions with a dynamic range of $\sim 10^5:1$ and provide distribution information to $>5X$ to $7X$ times typical rms-beam widths. Table 1 summarizes Figs. 3 and 4 distributions' statistical beam-width information. Note how the FW10%M and FW1%M show the added distribution “shoulder” widths resulting from beam mismatched condition whereas the FWHM actually shows a slight decrease in beam width.

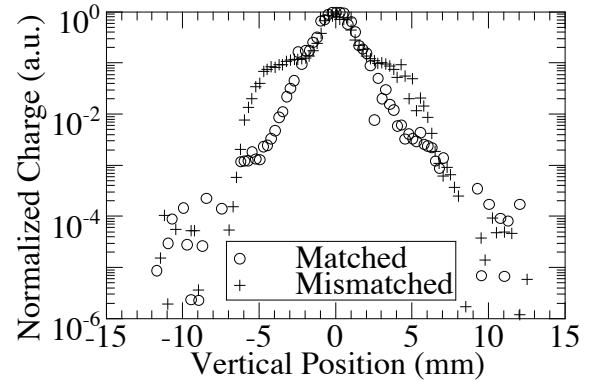


FIGURE 3. Acquired vertical beam distributions from WS/HS #51 show “shoulders” resulting from a beam mismatch condition.

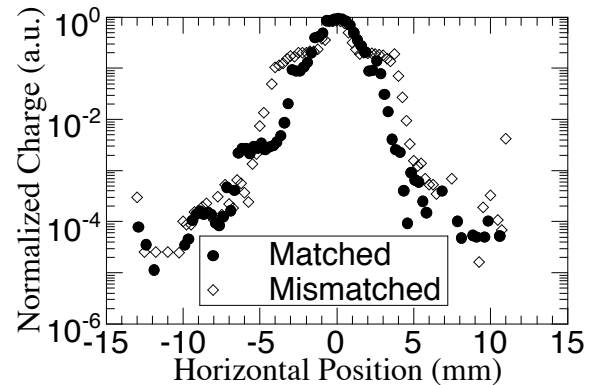


FIGURE 4. Acquired horizontal beam distributions from WS/HS #51 show “shoulders” resulting from a beam mismatch condition.

Table 1. Distribution width statistics, such as FW10%M, can further describe “shoulders” in the mismatched profile beam data shown in the Figs. 3 and 4 data.

Width (mm)	Vertical Mtchd.	Vertical Msmtchd.	Horizontal Mtchd.	Horizontal MsMtchd.
R.m.s. Width	1.15	1.89	1.10	1.82
FWHM	2.29	1.92	2.13	1.56
FW10%M	4.46	7.21	4.41	8.06
FW1%M	7.48	11.92	6.70	9.48

WIRE AND SCRAPER PHYSICS

The WS wire is biased negative to optimize secondary emission (S.E.) yield, where the yield is defined as the ratio of the emitted secondary electron current and the proton beam current intercepted by the wire. All of the wires in the halo lattice WS are configured with a 33- μm , carbon monofilament. The HEBT WS is configured with a 100- μm SiC wire. The choice of bias potential was determined by measuring the wire and scraper currents as a function of bias potential. The resulting data showed that the wire is optimally biased at -6 to -12 V and the scraper is optimally biased at +20 to +30 V [4].

As the wire bias is positively increased from 0 V to > +100 V, the wire secondary electron emission is inhibited and the net wire current reduces to very near zero. As expected, a large positive bias reduces the wire detection signal. Furthermore, it appears that the wire collects positive ions with < -25 V bias potentials well after the beam pulse. This ion collection additionally limits the amount of negative bias that is applied to the wire for proper secondary emission operation.

The scraper detection goal is to inhibit secondary emission and detect only 6.7-MeV protons. With approximately +25 V bias applied to the scraper, the secondary emission is almost entirely inhibited and the net current reduces to the nominal proton current.

SUMMARY

A wire scanner and halo scraper have been integrated into a single beam profile instrument capable of $10^5:1$ dynamic range. This WS/HS combination was used extensively to acquire wide dynamic range data in order to understand beam halo generation. The WS/HS beam data were analyzed under matched and mismatched beam conditions. Statistics, such as FW10%M, further described the irregular-shaped beam distributions resulting from

mismatch beam conditions. The scanner and scraper V-I curves showed that the wire and scraper are optimally biased at -12 V and +25 V, respectively.

REFERENCES

1. J. D. Gilpatrick, et al., “Experience with the Low Energy Demonstration Accelerator (LEDA) Halo Experiment Beam Instrumentation,” *Proceedings of the 2001 Particle Accelerator Conference*, June 18-22, 2001, pp.2311-2313.
2. T. Wangler, “Physics Results from the Los Alamos Beam-Halo Experiment,” this workshop.
3. P. L. Colestock, et al., “Measurement of a Beam Halo Generation in an Intense Proton Beam,” *20th ICFA Advanced Beam Dynamics Workshop on High Intensity and High Brightness Hadron Beams*, Fermilab National Laboratory, April, 8-12, 2002.
4. J. D. Gilpatrick, et al., “Biasing Wire Scanners and Halo Scrapers for Measuring 6.7-MeV Proton-Beam Halo,” *Proceedings of the 2002 Beam Instrumentation Workshop* held at Brookhaven National Laboratory, on May 6-9, 2002.